



## The Effect of Deposition Temperatures on the Structural and Optical Properties of CuZnS Thin Films

Layth A. Saleh\* and Ziad T. Khodair

Department of Physics – College of Science – University of Diyala

[34605@gmail.com](mailto:34605@gmail.com)

Received: 3 July 2022

Accepted: 22 September 2022

DOI: <https://dx.doi.org/10.24237/ASJ.01.02.644B>

### Abstract

The structural and optical characteristics of thin CuZnS films were examined in this research. The films were created utilizing the spin coating technique at different temperatures (200, 250 and 300 °C). According to XRD investigations, all compounds showed a polycrystalline structure with a hexagonal structure. The field emission scanning electron microscopy, surface morphology were investigated (FE-SEM). As the temperature is raised, the average particle size increases. The absorption spectra of CuZnS thin films showed that, for all samples, absorption increases as temperature rises for all samples. The optical characteristics of the material, including absorbance and absorbance coefficient, were investigated as well.

**Keywords:** Thin Film, Spin coating, Optical Properties, absorbance coefficient.



## تأثير درجات حرارة الترسيب على الخصائص التركيبية والبصرية لأغشية CuZnS الرقيقة

ليث علي صالح وزباد طارق خضير

قسم الفيزياء – كلية العلوم – جامعة ديالى

### الخلاصة

في هذا البحث تم فحص الخصائص التركيبية والبصرية لأغشية CuZnS الرقيقة، تم إنشاء الأغشية باستخدام تقنية الطلاء البرمي في درجات حرارة مختلفة (200، 250، 300 درجة مئوية). وفقاً لفحوصات XRD، أظهرت جميع المركبات تركيب متعدد التبلور ذات تركيب سداسي. باستخدام المجهر الإلكتروني الماسح الباعث للمجال (FE-SEM)، تم التحقيق في مورفولوجيا السطح. كلما ارتفعت درجة الحرارة، زاد متوسط حجم الجسيمات. تم فحص الخصائص البصرية كدالة للطول الموجي. توضح أطياف الامتصاص لأغشية CuZnS الرقيقة أنه بالنسبة لجميع العينات، تزداد الامتصاصية مع ارتفاع درجة الحرارة. كما تم فحص الخصائص البصرية للمادة، بما في ذلك الامتصاصية ومعامل الامتصاص.

**الكلمات المفتاحية:** الغشاء الرقيق، الطلاء البرمي، الخواص البصرية، معامل الامتصاص.

### Introduction

The CuS is an important semiconductor with distinctive typical electrical, chemical, and optical properties and a wide range of applications in solar cells. Recently, thin films CuS have demonstrated potential as gas-sensor materials [1]. According to structural and optical studies, CuS has a hexagonal structure and a direct bandgap of 2.36 eV and 2.03 eV [2]. Another important semiconductor known as (ZnS) by an energy band gap (3.65 eV) is the most significant value of all (II-VI) compound semiconductors with n-type semiconductors and a large direct bandgap. As a result, it can be applied to heterojunction solar cells as an anti-reflective coating and in optoelectronics [3]. Due to their modern techniques, nanocomposite thin films have recently gained interest for their structural, morphological, and optical characteristics. A Potential nanostructured material for photovoltaic cells, electroluminescent and photoconductor devices, and other optical device applications includes CuZnS ternary complexes. The nanocomposite films can also be used in solar cells as an absorber. Since the



brilliant p-type inorganic materials have a broad direct bandgap and are crucial for solar cell applications, improving the characterization of copper-zinc sulfide (CZS) with a direct wide-bandgap [4]. There are several methods to make CuZnS thin films, such as pyrolysis by spray [5, 6] and SILAR [7]. The CuZnS thin film was produced in the current work using the spin coating technique to study the structural and optical properties.

## **Experimental procedure**

The (CuZnS) was made by dissolving aqueous copper chloride  $\text{Cu}_2\text{Cl}_2 \cdot 2\text{H}_2\text{O}$  at a concentration of (2M) as a source for copper ions, zinc chloride at a concentration of (2M) ( $\text{ZnCl}_2$ ) as a source for zinc ions, and thiourea  $\text{Sc}(\text{NH}_2)_2$  at a concentration of (4M) as a source for sulfur ions in a final volume of 5 ml of 2-methoxy ethanol anhydrous. The mixture is stirred at (50 °C) using a (magnetic stirrer) for a period of time (10 min). Then, 0.05 ml of mono-Ethanolamine was added drop by drop to control the alkalinity of the solution and achieve complete solubility of the compounds; after 5 minutes on the magnetic stirrer at the same temperature, the solution is clear and residue-free. The pH-Value was found to be identical (pH = 7). The final mixture color was homogeneous. A spin coater type (L2001A3, Ossila, UK) with speed and time settings that can be adjusted from 100 to 6000 rpm and 1 to 1000 seconds was used in this study. A Micrometers to nanometers in thickness can be achieved using the spin coating process. A Deposition, spin-up, spin-off, and evaporation are all shown in Figure 3.6, the samples are heated to temperatures of (200, 250, and 300 °C). This heat treatment process removes organic residues (organic contamination) and undesirable elements (remains of solution components).

## **Results and discussion**

### **Structural properties**

The XRD patterns are shown in Figure 1 of CuZnS thin film prepared by spin coating at different deposition temperatures of 200, 250, and 300 °C. A CuZnS at 200°C Diffraction peaks show in the pattern around ( $2\theta \sim 26.0891^\circ, 28.5553^\circ, 29.9234^\circ, 46.1691^\circ, \text{ and } 57.1857^\circ$ ) corresponding to (100), (101), (102), (110), and (311), All films have a hexagonal structure with lattice parameters of  $a=b=3.87 \text{ \AA}$  and  $c=5.60 \text{ \AA}$ . The pattern has diffraction peaks around

( $2\theta \sim 26.2788^\circ$ ,  $28.5752^\circ$ ,  $29.4041^\circ$ ,  $46.1196^\circ$ , and  $57.1357^\circ$ ) when CuZnS is formed as a thin film at  $250^\circ\text{C}$  which correspond to (100), (101), (102), (110) and (311). All films have a hexagonal structure with lattice parameters of  $a=b=3.86\text{ \AA}$  and  $c=5.64\text{ \AA}$ . For CuZnS thin film deposition at  $300^\circ\text{C}$ , the pattern shows diffraction peaks around ( $2\theta \sim 26.4086^\circ$ ,  $28.6801^\circ$ ,  $29.1619^\circ$ ,  $46.6493^\circ$ , and  $57.3681^\circ$ ), corresponding to (100), (101), (102), (110), and (311), and the films have a hexagonal structure with lattice parameters of  $a=b=3.86\text{ \AA}$  and  $c=5.61\text{ \AA}$ . Peaks on the XRD pattern match those on the International Center of Diffraction Data (ICDD) card (80-0007 & 06-0464). The highest point is at  $2\theta \sim 29^\circ$ , corresponding to the (102) plane. This finding is consistent with Ghamdan M.M. Gubari et al. [8] extremely well. Notably, the XRD pattern favored the (102) plane, with thin peaks and high intensity. This demonstrates the well-defined crystallinity of CZS if it is nano, it is nanostructure and nanoparticle [9]. From these spectra, structural data such as the diffraction angle ( $2\theta$ ), lattice spacing ( $d$ ), full width at half maximum (FWHM), phases, and hkl planes were computed and displayed in Table 1.

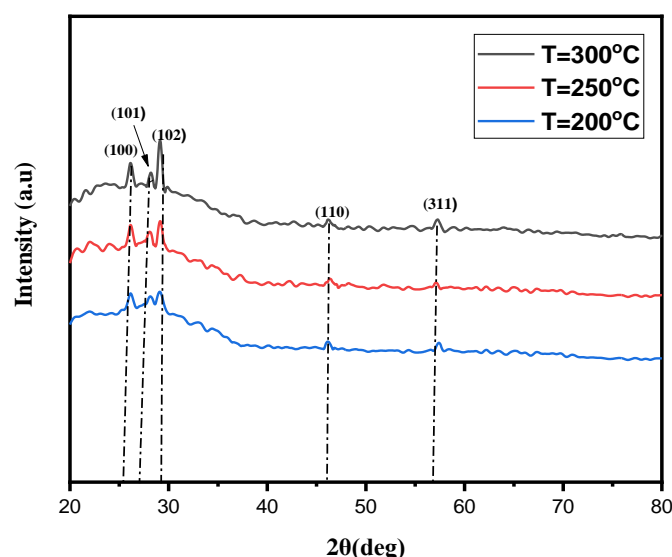


**Figure 1:** X-ray Diffraction of CuZnS thin films at different substrate temperatures (200, 250, and  $300^\circ\text{C}$ ).



**Table 1:** Structural characteristics of CuZnS at different substrate temperatures (200, 250, and 300 °C).

Thin Films	Temperature ° C	2θ (deg)	d-spacing	hkl	FWHM (deg)
Cu Zn S	200	26.0891	3.36481	100	0.92000
		28.5553	3.17342	101	0.57000
		29.9234	2.96784	102	0.52000
		46.1196	1.95760	110	0.48000
		57.1857	1.59580	311	0.76000
	250	26.2788	3.35124	100	0.87300
		28.5752	3.17021	101	0.37000
		29.4041	2.98037	102	0.32000
		46.1691	1.95717	110	0.26000
		57.1357	1.59477	311	0.68000
	300	26.4086	3.36233	100	0.78000
		28.6801	3.16829	101	0.27000
		29.1619	2.98365	102	0.23000
		46.6493	1.95697	110	0.26000
		57.3681	1.593649	311	0.38000

## Structural parameter

### Average Crystallite Size ( $D_{av}$ )

By the Scherrer equation [10,11] obtained from the relationship (1), The average crystallite size was calculated, revealing that as the temperature rises, all CuZnS films exhibited improved order crystallinity and revealed that with increasing temperature, all CuZnS films showed improvement in crystallinity.

$$D_{av} = \frac{K \lambda}{\beta \cos \theta} \dots\dots\dots (1)$$

where  $\theta$  is the Bragg diffraction angle, K is the shape factor, which ranges from 0.9 to 1 depending on the material's shape, and the Full Width at Half Maximum (FWHM), is expressed in radians.

### FE-SEM Results

The surface morphology and microstructure features of deposited thin films were investigated by a field emission scanning electron microscope (FE-SEM). To investigate the surface of the thin films, FE-SEM images of CuZnS films were attained for analysis (Figure 2). At temperatures (200, 250, and 300 °C) within the nano-scale range, the surface structure of the

thin film matched the form of a Cauliflower without a change in its thickness or profile. According to the grain distribution diagram, the grain size of CuZnS films increases as substrate temperature rises. The collected results are virtually identical to the researchers' findings [12].

**Table 2:** Values of smallest and largest particle size and average particle size of the prepared films.

Sample	Temperature °C	Average size (nm)	Minimum Size (nm)	Maximum Size (nm)
CuZnS	200	82.75	34.21	185.79
	250	108.50	33.42	230.88
	300	157.95	54.74	356.33

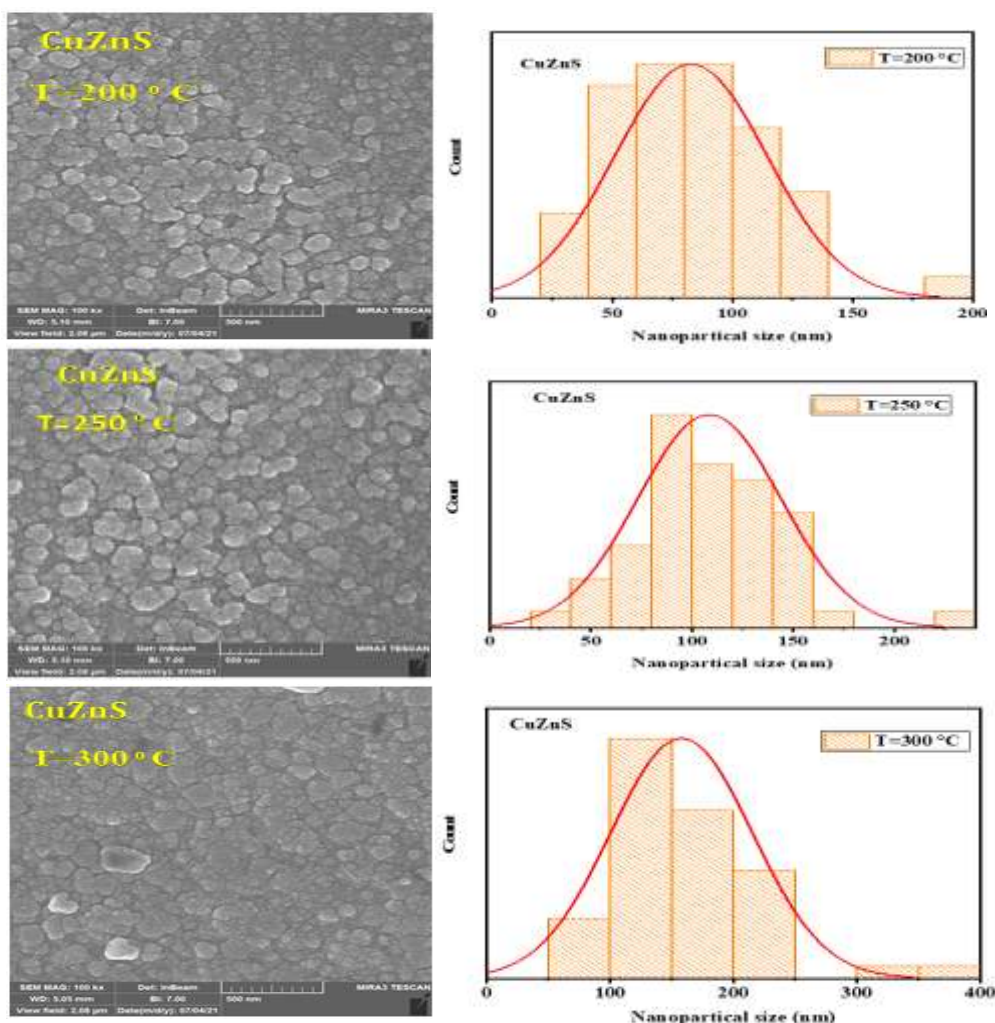


**Figure 2:** FE- SEM images for CuZnS and planner volumetric distribution



## Optical properties

### Absorbance (A)

Figure 3 depicts the variation in CuZnS thin film absorbance as a function of wavelength between 300 and 900 nm. with the substrate temperature increases, the absorbance spectra of CuZnS thin films reveal prominent absorption edges. Indicates that an increase in substrate temperature might enhance the crystallinity of CZS [13, 14].

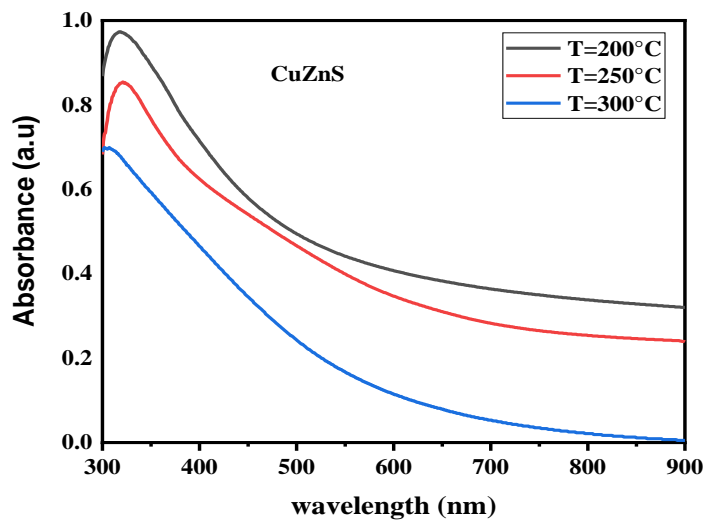


**Figure 3:** The absorbance for CuZnS thin films at different substrates temperature (200, 250, and 300 °C).

### Absorption Coefficient ( $\alpha$ )

The following equation was used to compute the absorbance coefficient of nanostructured (CuZnS) thin films [15]:

$$\alpha = 2.303 \frac{A}{t} \dots\dots\dots (2)$$

where, A is the absorption, and is the thickness of the film (cm).

Figure 1.4 demonstrates that CuZnS films have a high absorption coefficient ( $>10^4$ )  $\text{cm}^{-1}$  and that the absorption coefficient increases as the substrate temperature increases, which can be attributed to the increased crystallinity of the film [14].

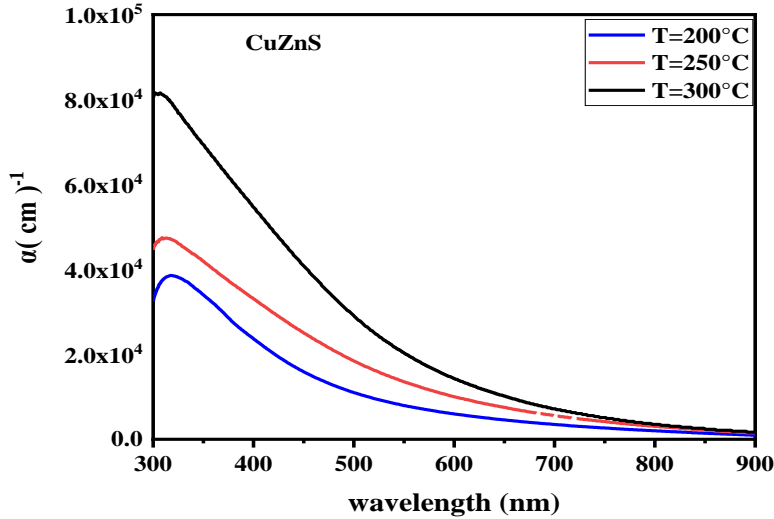


**Figure 4:** Variation of absorption coefficient versus photon energy  $Cd_2SnO_4$  at different substrate temperatures (200,250, and 300 °C).

For the film that was deposited, the direct band-gap value was determined using the relationship (3) [16, 17]. The energy gap value ( $n = 1/2$ ) is 2.25eV at ( $T=200$  °C), decreasing to 1.94 eV at ( $T=250$  °C) and 1.80 eV at ( $T=300$  °C). This drop in the band gap of films after increasing the substrate temperature may be a result of an increase in crystallinity, as evidenced in the XRD pattern, and it was found the band gap rate of CZS nanoparticles fell as copper concentration increased [18].

$$\alpha(h\nu) = A (h\nu - E_g)^n \dots\dots\dots (3)$$

where,  $h\nu$  is the photon energy,  $A$  is a constant depending on the material's structure,  $E_g$  is the optical band gap of the samples, and  $n = 1/2$  for direct band gap and 2 for indirect band gap.

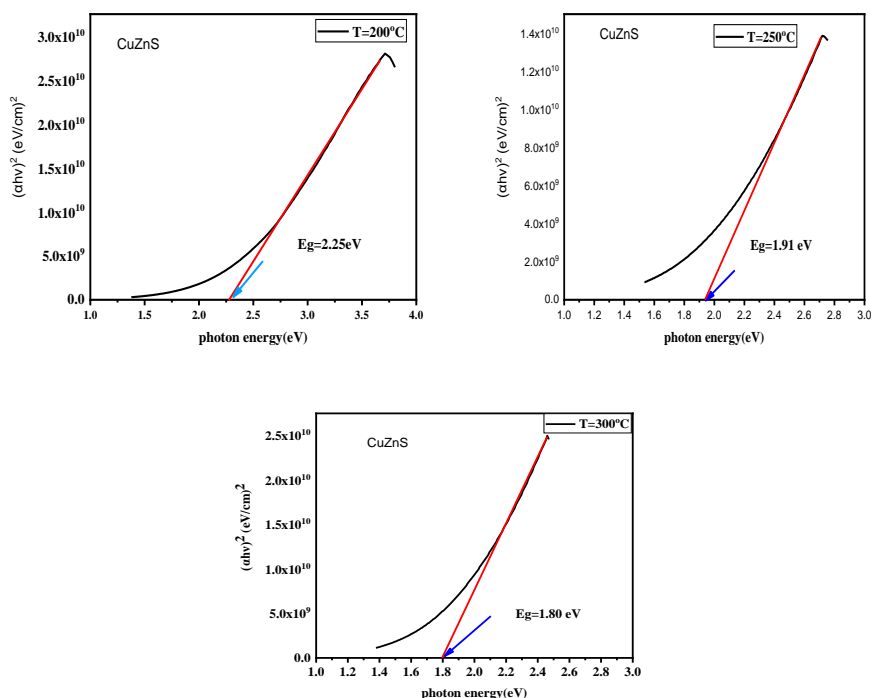


**Figure 5:**  $(\alpha h\nu)^2$  as a function of energy photon for nanostructure CuZnS thin films deposited at different substrate temperatures (200, 250, and 300 °C).

## Conclusions

The spin coating technique is excellent for depositing CuZnS thin films on glass substrates; based on structural and optical properties, the elevated temperature operation improves the crystalline quality of the thin film. All films have a nanostructure that is hexagonal and polycrystalline. According to XRD and FE-SEM, when the substrate temperature increases, the average grain size of the nanoparticle thin film increases. The direct energy band gap decreases to 1.80 eV for the film deposited at 300 °C.



## References

1. M. A. Yıldırım, Optics Communications, 285(6),1215-1220(2012)
2. M. A. Yildirim, A. Ateş, A. Astam, Physica E: Low-dimensional Systems and Nanostructures, 41(8), 1365-1372(2009)
3. A. Ates, M. A. Yıldırım, M. Kundakçı, A. Astam, Materials Science in Semiconductor Processing, 10(6), 281-286(2007)
4. Khalil, A. A. I., A. S. H. Abd El-Gawad, Gadallah, A.S., Optical Materials, 109, 110250
5. M. S. Sreejith, D. R. Deepu, C. S. Kartha, K. Rajeevkumar, K.P. Vijayakumar, Applied Physics Letters, 105(20), 202107(2014)
6. M. Adelifard, H. Eshghi, M. M. B. Mohagheghi, Optics Communications,285,(21-22),4400-4404(2012)
7. M. A. Yıldırım, Optics Communications, 285(6), 1215-1220(2012)
8. G. M. Gubari, N. P. Huse, A. S. Dive, R. Sharma, Synthesis and characterization of structural, morphological and photosensor properties of Cu<sub>0.1</sub>Zn<sub>0.9</sub>S thin film prepared by a facile chemical method, In: AIP Conference Proceedings ,1953(1), 100014(2018)
9. S. K. Sundaram, S. Subramanian, V. Panneerselvam, and S. T. Salammal, Thin Solid Films, 733,138810(2021)
10. Ziad T. Khodair, Ali M. Mohammad, Anees A. Khadom, Chemical Data Collections 25, 100315(2020)
11. A. H. Abed, Z. T. Khodair, T. M. Al-Saadi, T. A. Al-Dhahir, Study the evaluation of Williamson–Hall (WH) strain distribution in silver nanoparticles prepared by sol-gel method, 2123, AIP Publishing LLC, 020019(2019)
12. M. A. Yıldırım, Optics Communications, 285(6),1215-1220(2012)
13. Q. Chen, X. Dou, Y. Ni, S. Cheng, S. Zhuang, Journal of colloid and interface science, 376(1), 327-330( 2012)
14. S. K. Sundaram, S. Subramanian, V. Panneerselvam, S. T. Salammal, Thin Solid Films, 733, 138810(2021)
15. Z. T. Khodair, B. A. Ibrahim, M. K. Hassan, Investigation on the structural and optical properties of copper doped NiO nanostructures thin films, Materials Today: Proceedings, 20,560-565(2020)
16. S. A. Hameed, M. M. Kareem, Z. T. Khodair, I. M. M. Saeed, Chemical Data Collections, 33, 100677(2021)
17. M. M. Farhan, Z. T. Khodair, B. A. Ibrahim, Study of the Structural and Optical Properties of Ni-doped Co<sub>3</sub>O<sub>4</sub> Thin Films Using Chemical Spray Pyrolysis Technique, IOP Conf.Series: Materials Science and Engineering 871,012090(2020)
18. S. Rahaman, Y. M. G. Shenoy, V. N. Krishna, S. Shekhar, and H. Shaik, Effect of annealing on the properties of Cu<sub>2</sub>SnS<sub>3</sub> thin films using spin coating,2105(1), 020001(2019)